ELSEVIER

Journal of Photochemistry and Photobiology A: Chemistry 130 (2000) 157–162

Journal of Photochemistry and Photobiology A:Chemistry

www.elsevier.nl/locate/jphotochem

Photocatalysed degradation of uracil in aqueous titanium dioxide suspensions: mechanisms, pH and cadmium chloride effects

Christel Jaussaud [a], Olivier Païssé [b], René Faure [a,*]

[a] *Laboratoire d'Instrumentation et de Chimie Analytique en Solution (LICAS), Bât. 305, Université Claude Bernard Lyon 1, 69622, Villeurbanne cedex, France*

[b] *Service Central d'Analyse du CNRS, BP 22, 69390, Vernaison, France*

Received 8 October 1999; accepted 13 October 1999

Abstract

Upon UV irradiation, in O_2 saturated aqueous titanium dioxide suspensions, uracil is almost completely mineralised. Most of the organic compounds occurring during the photodegradation process have been identified by means of liquid chromatography and mass spectrometry coupled techniques (LC–MS). The first step of the mineralisation leads to the formation of uracilglycol. Then, the main products generated during the photodegradation exhibit new functions such as polyol, carboxylic and aldehyde. The presence of urea has been clearly evidenced. At the end of the process, the ultimate step is the formation of nitrate and ammonium ions. The formation kinetics of intermediate products are modified by pH variation and $CdCl_2$ addition.

Keywords: Uracil; Titanium dioxide; Photodegradation; Mechanism; Photocatalysis

1. Introduction

Pyrimidine derivatives are present in continental water [1], as well through natural DNA biodegradation as pollution effects such herbicide uses. All these compounds may be considered as water pollutants. Photocatalytic reactions on semiconductor powders (TiO_2, ZnO, CdS) are very hopeful in the removal of these compounds [2,3]. Such processes may be directly involved in aquatic environments leading to intermediate species before a final mineralisation.

The efficiency of the photocatalytic mineralisation is strongly dependent on the experimental conditions such as pH, oxygen concentration and, presence or absence of metallic ions [4]. Among the various available semiconductors, TiO_2 appears to be the most widely employed due to its good degradation effect. A recent overview shows that the titanium dioxide features predominantly in past and present works on semiconductor photocatalysis [5].

The uracil degradation has been previously investigated, since this molecule may be considered as a model in the pyrimidine series. In the case of TiO_2 assisted photo-oxidation of uracil, the initial rate was found almost constant at all pH values [6]. In the simultaneous presence of Ag^+, the kinetics depends on the metallic concentration showing a maximum efficiency for a $[Ag^+]$/[uracil] ratio of 3 [6]. The use of an other photocatalyst such as ZnO leads to results similar to those obtained with TiO_2 [7].

The degradation mechanism has already been partially elucidated. At the beginning of the degradation, a dichloromethane solvent extraction of the medium has evidenced, by IR spectrometry, the presence of uracilglycol [6]. The final steps of mineralisation were determined by kinetics studies of NH_4^+ and NO_3^- formations at the end of uracil photocalysed process [8]. More recently, a primary amine was identified at the same time as NH_4^+, NO_3^-, N_2 and CO_2 during the TiO_2 photodegradation of uracil [9].

Herein we report the influence of pH and $CdCl_2$ pollutant presence on the photocatalysed TiO_2 uracil degradation. Moreover, the aim of the present work is to determine the nature of the uracil photoproducts in order to propose a photochemical degradation mechanism.

2. Experimental

2.1. Materials

Uracil was a Janssen Chimica product with a 99% minimal purity. For all the experiments, the initial uracil con-

* Corresponding author. Tel.: +33-4724-31153; fax: +33-4724-46202.
E-mail address: faure@univ-lyon1.fr (R. Faure).

1010-6030/00/$ – see front matter
PII: S1010-6030(99)00212-9

centration was of 10^{-3} mol l^{-1}. For the tests in presence of metallic ions, cadmium chloride hemipentahydrate (Aldrich product, 98% minimal purity) was introduced at a concentration of 5×10^{-4} mol l^{-1}. The pH was adjusted by addition of hydrochloric acid (Fluka 32%) or sodium hydroxide (Prolabo Normapur). The photocatalyst compound, at a concentration of 0.5 g l^{-1}, was the titanium dioxide 'Degussa P25' which is predominantly anatase (80% anatase, 20% rutile). It is not porous, and presents a specific surface area of about 55 m^2 g^{-1} and a density of 3.85 g cm^{-3}.

Six runs of experiments were studied during this work in order to evidence pH and $CdCl_2$ effects: three same uracil solutions were submitted to photodegradation at pH 4, 6 and 8, respectively; three others were studied in presence of $CdCl_2$ at the three previous pH values.

2.2. Methods

The irradiation of the suspensions were carried out with a HPK 125 W Philips mercury lamp, emitting in the wavelength range 250–450 nm, with a maximum emission at 360 nm. The lamp was immersed in a 2 l photoreactor by means of a Pyrex-glass hole cutting the radiation shorter than 290 nm. The well-closed reactor was cooled by circulating water. The solution was stirred by magnetic stirrer and the reaction occurred in the presence of oxygen bubbled through the solutions at a flow rate of 6 l h^{-1}. The advance of the reaction was followed by sampling during the degradation process. Each sample was immediately centrifuged at $2000 \times g$ for 15 min and was firstly filtered on 0.45 μm Whatman filter and successively on 0.22 μm one to eliminate the TiO_2 particles.

The uracil degradation was followed by high performance liquid chromatography (hplc) (Shimadzu LC-10AS) using a Nucleosil C18 column, ultra pure water (Elga) as mobile phase and UV detection at 270 nm corresponding to the highest absorption wavelength of the uracil.

The intermediate products were separated and identified by means of an LC-MS (HP 1100 series LC MSD) with a Chrompack C18 Inertsil ODS3 (5 μm − 150 mm × 3 mm) column + a precolumn (10 mm × 3 mm). The mobile phase was made of formic acid in water, pH adjusted at 2.45 with a pH-meter. The UV detection was monitored from 210 to 260 nm and was fixed finally to 210 nm corresponding to the maximal absorption of most intermediate molecules. A post-column addition, using an external pump, of a 50/50 mixture of isopropanol and ammonium formate (1 mM, pH adjusted at 7.8 with diluted ammoniac) in order to improve the chemical ionisation and the nebulization of the eluted compounds in the source interface. Mass spectrometry detection was realised in positive and negative electrospray mode.

Inorganic ions were analysed by means of capillary electrophoresis (Q4000 Waters). The applied potential was around 15 kV. Injections were realised in hydrostatic mode during 30 s. For anion analysis, the detection was in reverse UV at 254 nm and the electrolyte was the OFM-OH^- of Waters. For cation analysis, detection was realised in reverse UV at 185 nm and the electrolyte was the UV-CAT2 of Waters.

3. Results and discussion

3.1. Uracil disappearance

The pH influence was tested around the TiO_2 Zero Point of Charge (pH 6.4). In the range pH 4–pH 8, the uracil disappearance kinetics increases with pH [Fig. 1], according to a $OH^\bullet$ attack leading in a first step to uracilglycol [6,7]. The formation of $OH^\bullet$ depends on the solution pH value. In acidic and neutral solution [10,11] the reaction is $H_2O + h^+ \rightarrow OH^\bullet + H^+$. In alkaline solution, the generation of the radical $OH^\bullet$ is easier than in neutral and acid solution [12]: $OH^- + h^+ \rightarrow OH^\bullet$ [13].

3.2. Identification of degraded uracil compounds

All the intermediate molecules were identified from LC–MS either by positive electrospray mode (ES+) or negative electrospray mode (ES−). Hereunder are listed the different compounds involved in the proposed mechanism and each is referenced by its product number (Scheme 1) and its retention time (tr):

(**1**) tr = 8.1 min, ES+, m/z = 113 [M + H], m/z = 135 [M + Na]
(**4**) tr = 10.4 min, ES−, m/z = 145 [M − H]
(**6**) tr = 3.2 min, ES+, m/z = 165 [M + H] ,
(**7**) tr = 3.7 min, ES−, m/z = 159 [M − H], m/z = 141 [M–H–H_2O], m/z = 115 [M–H–COO]
(**8**) tr = 6.0 min, ES−, m/z = 143 [M − H]
(**9**) tr = 4.0 min, ES−, m/z = 115 [M − H]
(**10**) tr = 5.2 min, ES−, m/z = 133 [M − H], m/z = 87 [M–$CH(OH)_2$]
(**11**) tr = 5.4 min, ES−, m/z = 87 [M − H]
(**13**) tr = 3.5 min, ES−, m/z = 181 [M − H],m/z = 145 [M–H–$2H_2O$]
(**14**) tr = 4.2 min, ES−, m/z = 151 [M − H]
(**15**) tr = 6.4 min, ES+, m/z = 124 [M + H]
(**16**) tr = 6.4 min, ES+, m/z = 108 [M + H]
(**17**) tr = 3.4 min, ES+, m/z = 61 [M + H]

3.3. Proposed mechanism

The $OH^\bullet$ attack of the double bond C_5–C_6 leads to the uracilglycol (**4**) via the two radical species (**2**) and (**3**). The uracilglycol formation was previously evidenced [6,7] and the $OH^\bullet$ attack on C5 and C6 is in accordance with the maximum of the frontier electron densities calculated using the CAChe (MOPAC) system [9].

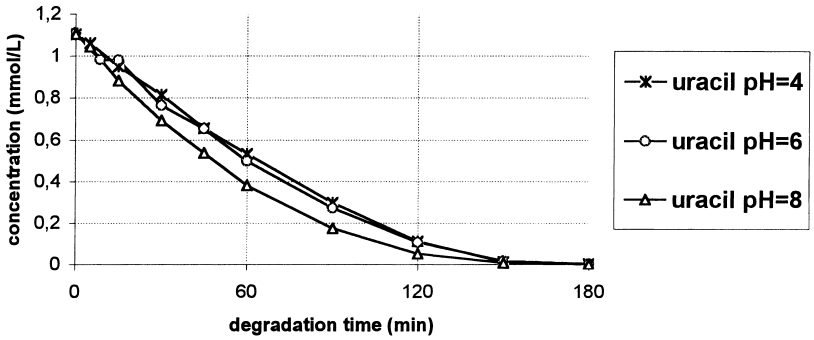

Fig. 1. Uracil disappearance kinetics at pH 4, 6 and 8.

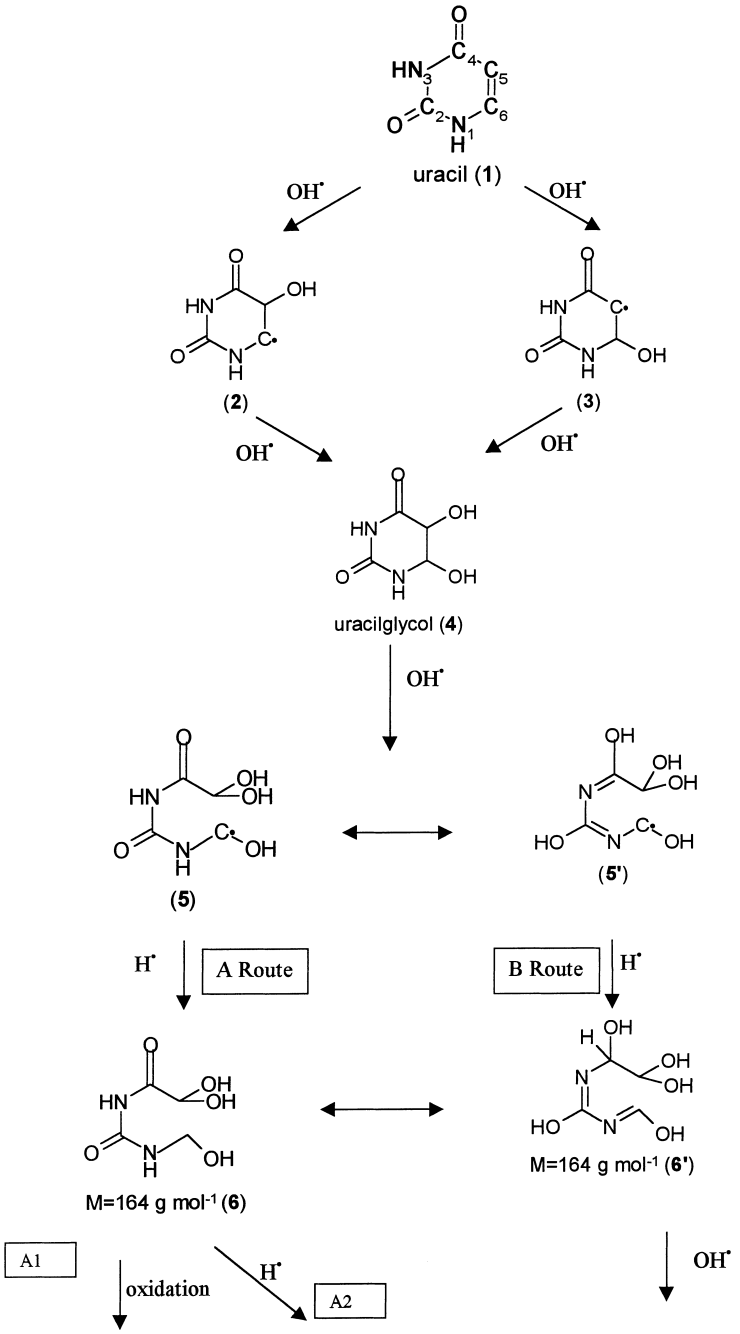

Scheme 1. Proposed mechanism for the uracil photodegradation.

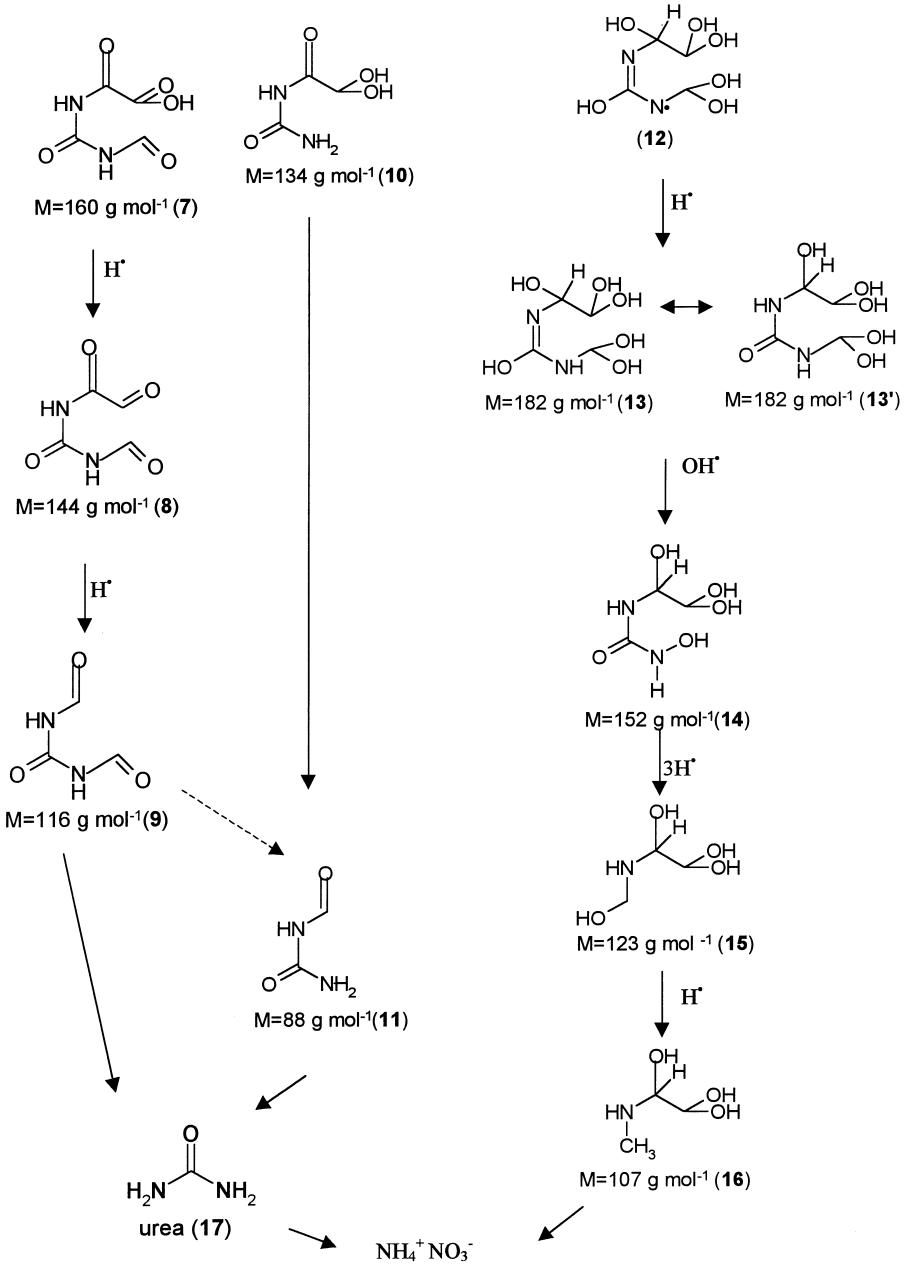

Scheme 1 (*Continued*).

The next step involves the heterocycle opening of the uracilglycol. The preferential route is the attack of C_5–C_6 [14,15] leading to the radical (**5**) which may be stabilised by the resonant form (**5′**). The radicals (**5**) and (**5′**) may interact with a $H^{\bullet}$ giving to rise respectively (**6**), A route, and (**6′**), B route.

For the A route, from (**6**), there is two ways A1 and A2. In the first way, two alcoholic functions (at C_5 and C_6) of (**6**) may be oxidised leading to an aldehydic function at C_6 and a carboxylic function at C_5 ((**7**), $M = 160$). It is noteworthy that the photolysis of the pyridine leads to a hydroxylated pyridine where the heterocycle is opened with production of an aldehydic function [16]. Owing to the compound (**7**) shows a COOH function adjacent to a CO group, the $OH^{\bullet}$ attack could be a way for the obtention of oxalate ion. Nevertheless, this species was never evidenced by capillary electrophoresis whatever the irradiation time. In fact, (**7**) is decomposed by $H^{\bullet}$ attack, and leads to (**8**) ($M = 144$) showing two aldehydic functions. Such molecule was already identified for thymine photocatalysis [14] and uracil radiolysis [GC–MS technic, [15]]. A new $H^{\bullet}$ attack leads to a new dialdehyde (**9**) ($M = 116$) which is finally converted

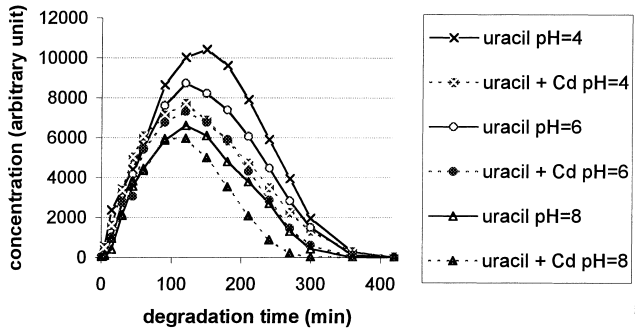

Fig. 2. Kinetics of formation-disappearance of the product (**6**) $M = 164\,g\,mol^{-1}$.

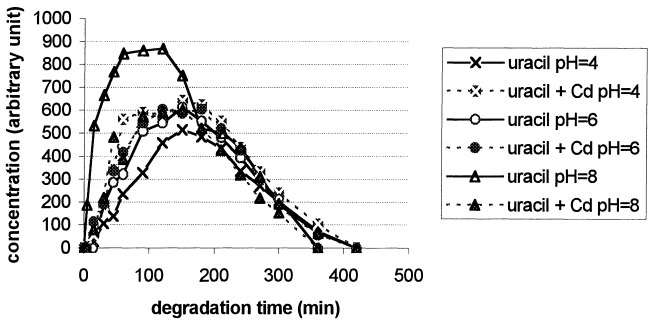

Fig. 3. Kinetics of formation-disappearance of the product (**9**) $M = 116\,g\,mol^{-1}$.

in urea (**17**) ($M = 60$) by means of an intermediate step (**11**) ($M = 88$). It is noteworthy that the experimental mass spectrum of (**17**) was indubitably confirmed by injection of urea in LC-MS. The second way to decompose (**6**) (way A2) is a $H^{\bullet}$ attack of the N_1–C_6 bond leading to (**10**) ($M = 134$). A new $H^{\bullet}$ attack of the C_4–C_5 leads to the same product (**11**) of the A1 route, and consecutively to the urea (**17**). The final degradation products of urea are NH_4^+ and NO_3^- [17].

For the B route, taking in consideration that the subsequent products ((**15**) $M = 123$ and (**16**) $M = 107$) have odd

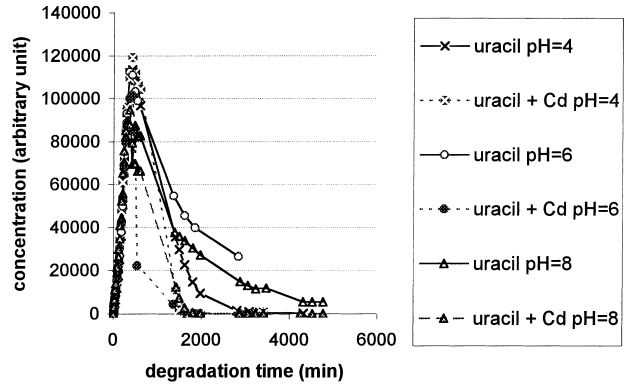

Fig. 4. Kinetics of formation-disappearance of the product (**11**) $M = 88\,g\,mol^{-1}$.

mass values, the degradation way implies necessarily one step with the loss of one nitrogen atom. The H attack of the resonant form (**5′**) leads to a resonant form (**6′**), and a subsequent $OH^{\bullet}$ attack, through the radical (**12**), leads, by a $H^{\bullet}$ attack to (**13**) and **13′** ($M = 182$). These last compounds by a $OH^{\bullet}$ attack lead to (**14**) ($M = 152$). From this molecule, by a $H^{\bullet}$ attack and the loss of N_1 is obtained the compound (**15**) ($M = 123$), and through a $H^{\bullet}$ attack, the molecule (**16**) ($M = 107$) which is mineralized in NH_4^+ and NO_3^- ions.

3.4. Kinetics of major intermediate products

The concentrations of three organic major compounds were registered during the degradation process in order to evaluate the influence of pH and $CdCl_2$ parameters. The Figs. 2–4 show the concentration curves of the three major products ($M = 164$, 116 and 88) versus irradiation time.

The pH and $CdCl_2$ parameters modify the kinetics of concentration variations of these three compounds. Nevertheless, the multistep processes don't allow to explain how theses parameters act on the mechanisms.

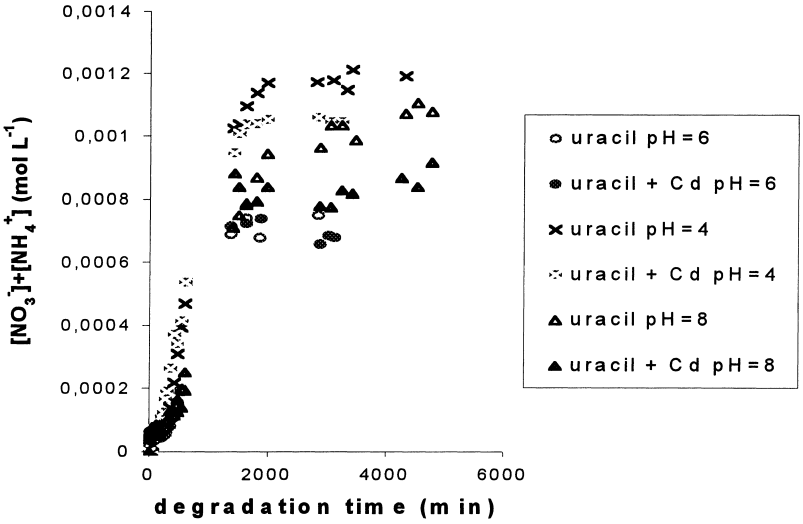

Fig. 5. Sum $[NO_3^-] + [NH_4^+]$ versus degradation time in the six conditions.

3.5. NO_3^- and NH_4^+ analyses

The concentration of NO_3^- and NH_4^+ measured by means of capillary electrophoresis allow to calculate the sum $[NO_3^-] + [NH_4^+]$ versus time for different conditions (Fig. 5).

All the concentration curves show the same kinetics during the first hours, but reach different final values. The final plateau height depends on the pH and $CdCl_2$ conditions. It is noteworthy that the highest final concentration (1.2×10^{-3} mol l^{-1}) does not agree with the calculated value for a complete degradation. This may be explained by N_2 formation and by incomplete degradation. It was not possible to detect N_2 by GC because of retention time of this compound is too similar to O_2 retention time and O_2 is at too high concentration. Nevertheless Horikoshi et al. [9] have detected the formation of N_2.

4. Conclusions

The LC–MS technic has allowed to identify the main products which are involved in the main degradation routes. Some of those compounds had been previously identified by other technics. It seems, despite of good conditions (photocatalyst and high UV irradiation), that the mineralisation is not achieved. Thus, in environmental medium, pyrimidine derivatives can be partially decomposed, giving mineral compounds such NO_3^- that may be considered as pollutant, but also giving organic compounds which seem stable during one or more hours.

References

[1] J.C. Moris, N. Ram, B. Baum, E. Wajon, Report to the US Environment Protection Agency, EPA, N°600 (1980) 2-80-031.
[2] M.A. Fox, M.T. Dulay, Chem. Rev. 93 (1993) 341.
[3] N. Serpone, E. Pelizzeti (Eds.), Photocatalysis: Fundamentals and Applications. Wiley, New York, 1989.
[4] V. Brezova, A. Blazkova, E. Borosova, M. Ceppan, R. Fiala, J. Mol. Catal., A: Chemical 98 (1995) 109.
[5] A. Mills, S. Le Hunte, J. Photochem. Photobiol., A: Chem. 108 (1997) 1.
[6] M.R. Dhananjeyan, R. Annapoorani, R. Renganathan, J. Photochem. Photobiol. A: Chem. 109 (1997) 147.
[7] R. Annapoorani, M.R. Dhananjeyan, R. Renganathan, J. Photochem. Photobiol. A: Chem. 111 (1997) 215.
[8] J.L. Lucas Vaz, A. Boussaoud, Y. Ait Ichou, M. Petit-Ramel, Analusis 26 (1998) 83.
[9] S. Horikoshi, N. Serpone, S. Yoshizawa, J. Knowland, H. Hidaka, J. Photochem. Photobiol. A: Chem. 120 (1999) 63.
[10] A. Fujishima, K. Honda, J. Chem. Soc. Japan 74 (1971) 355.
[11] A. Fujishima, K. Honda, Nature 238 (1972) 37.
[12] Z. Shourong, H. Quigguo, Z. Jun, W. Bingkun, J. Photochem. Photobiol. A: Chem. 108 (1997) 235.
[13] S. Sato, J.M. White, J. Am. Chem. Soc. 102 (1980) 7206.
[14] B. Ohtani, H. Nagasaki, K. Sakano, S.I. Nishimoto, T. Kagiya, J. Photochem. Photobiol. A: Chem. 41 (1987) 141.
[15] M.N. Schuchmann, C. von Sonntag, J. Chem. Soc. Perkin Trans. II (1983) 1525.
[16] J. Joussot-Dubien, J. Houdard, Tetrahedron Lett. 44 (1967) 4389.
[17] K. Nohara, H. Hidaka, E. Pelizzetti, N. Serpone, J. Photochem. Photobiol. A: Chem. 102 (1997) 265.